Eur. Phys. J. D **39**, 415–422 (2006)
DOI: 10.1140/epjd/e2006-00113-4

THE EUROPEAN PHYSICAL JOURNAL D

Morphological differences between Bi, Ag and Sb nano-particles and how they affect the percolation of current through nano-particle networks

A.D.F. Dunbar[a], J.G. Partridge, M. Schulze, and S.A. Brown

Department of Physics and Astronomy, University of Canterbury, Private Bag 4800, Christchurch, New Zealand

Received 25 July 2005 / Received in final form 15 February 2006
Published online 18 May 2006 –

Abstract. Nano-particles of Bi, Ag and Sb have been produced in an inert gas aggregation source and deposited between lithographically defined electrical contacts on SiN. The morphology of these films have been examined by atomic force microscopy and scanning electron microscopy. The Bi nano-particles stick well to the SiN substrate and take on a flattened dome shape. The Ag nano-particles also stick well to the SiN surface; however they retain a more spherical shape. Whereas, many of the Sb nano-particles bounce off the SiN surface with only a small fraction of the Sb nano-particles aggregating at defects resulting in a non-random distribution of the clusters. These nano-scale differences in the film morphology influence the viability of applying percolation theory to in situ macroscopic measurements of the film conductivity, during the deposition process. For Bi and Ag nano-particles the increase in conductivity follows a power law. The power law exponent, t, was found to be 1.27 ± 0.13 and 1.40 ± 0.14, for Bi and Ag respectively, in agreement with theoretical predictions of $t \approx 1.3$ for 2D random continuum percolation networks. Sb cluster networks do not follow this model and due to the majority of the Sb clusters bouncing off the surface. Differences in the current onset times and final conductance values of the films are also discussed.

PACS. 73.63.-b Electronic transport in nanoscale materials and structures – 36.40.-c Atomic and molecular clusters – 64.60.Ak Renormalization-group, fractal, and percolation studies of phase transitions – 81.07.-b Nanoscale materials and structures: fabrication and characterization

1 Introduction

The inevitable future for electronics is to use single atoms or molecules as the building blocks in the assembly of devices. This goal has not yet been attained but there is considerable interest [1,2] in development of new techniques that will bridge the gap between molecular devices and the commercial fabrication techniques available today [3,4]. Devices made from clusters of atoms or molecules, i.e. nano-particles, may allow that gap to be bridged, since these building blocks are readily available in any size between 0.5 nm and 100 nm. Nano-particles also offer the potential to fabricate 'new' materials for devices with novel functions because they are known to display unusual behavior in their electrical, structural and other properties [1,2]. Therefore, electrically contacted films of nano-particles are of interest.

Percolation theory has been used to model critical phenomena in a wide range of systems [5]. It relates various properties of the system to the probability of occupation of sites within the system by simple power laws. For example, the correlation length ξ of connected structures is described by

$$\xi \propto (p - p_c)^{-\upsilon}, \tag{1}$$

where p is the probability of site occupation, p_c is the critical occupation probability at which percolation occurs in an infinite system and υ is the power law exponent for ξ. One of the reasons for the importance and widespread applicability of percolation theory is the predicted universality of the exponents [5,6]. While there have been extensive theoretical studies of percolation and power law behavior, experimental studies have been relatively rare. Previous work has shown that finite size effects in 2D Bi nano-particle films are in agreement with percolation theory [7].

In this work we describe the production of nano-particles of Ag, Bi and Sb, and their deposition onto SiN substrates with lithographically defined contacts. We investigate the morphology of the deposited nano-particles and perform in situ measurements of the conductivity of the percolating film of particles, therefore, we can relate the nano-scale properties of the films to their macroscopic conductivity.

[a] *Currently at*: The Department of Physics and Astronomy, The University of Sheffield, S3 7RH, UK.
e-mail: a.dunbar@sheffield.ac.uk

We experimentally determine the conductivity exponent t in the power law predicted by percolation theory

$$\sigma \propto (p - p_c)^t, \tag{2}$$

where σ is the conductivity of the nano-particle film, and compare the results to predicted values. In doing so we establish that for Ag and Bi nano-particles percolation theory is applicable to their deposition onto SiN substrates but this is not the case for Sb nano-particles. Therefore we demonstrate that the nano-scale morphology of such nano-particle films controls the macroscopic properties of these films.

2 Percolation theory

Within percolation theory the many different systems that can be studied may be classified into two types; either discrete, i.e. the constituents of the system are fixed at discrete sites of a regular lattice (an early example being Ref. [8]), or continuous, i.e. the constituents may locate at any random location within a continuum. Many researchers have studied percolation in discrete lattice systems, however much less work has been done on continuous systems. The 2D inverted Swiss-cheese model consists of randomly positioned 2D discs of conducting material on a non-conducting 2D surface, where the strength of connections between particles is non-uniform. It is an appropriate starting point when considering the electrical properties of nano-particle films on 2D surfaces. The value of p_c for the inverted Swiss cheese model, is reported [9] to be 0.676339.

Theoretical studies by Feng, Halperin and Sen (FHS) [10,11] have investigated the power law exponents for transport properties in continuous networks, and for the case of the 2D inverted Swiss-cheese model, they showed that the conductivity relation equation (2) should be universal i.e., the power law exponent t should take its universal value of $t \approx 1.3$. This theory was extended by Balberg [12] to allow for non random distribution of the size of the discs and spheres in 2D and 3D. Balberg concluded that the exponent t could have any value larger than its universal value, except in the case of 2D conducting discs where t always takes the universal value 1.3.

Several experimental papers have been published which report investigations of percolation in large systems. For example Okazaki et al. [13,14] used conducting ink to generate a 2D inverse Swiss-cheese model and measured its conductivity exponent t, which they found to be the same as that for their discrete 2D model. Dubson and Garland [15] used an $x - y$ plotter to scribe holes in an aluminium sheet and measured the conductivity of the perforated sheet. They found the conductivity exponent t to be 1.34 ± 0.07 for their random void continuum.

Although a limited number of experimental studies of percolating nano-particle systems have been previously carried out the power law behavior predicted by equation (2) has not been confirmed in these systems. Yamamuro et al. [16] deposited 6–13 nm cobalt particles and concluded that the power law exponent increased with increasing particle size and did not follow a simple scaling law. They attributed this non-universality to overlapping of and ferromagnetic attraction between the Co particles. Melinon et al. [17] compared the deposition of Sb_4 molecules and Sb_{1850} particles (4.8 nm diameter) on glass substrates. They found that there was considerable diffusion and nucleation for the Sb_4 deposition, resulting in the formation of much larger particles and a critical coverage for percolation considerably larger than the theoretical value. For the Sb_{1850} particles there was minimal diffusion and nucleation, resulting in a percolating network consistent with a simple site percolation model. Schmelzer et al. [7] deposited bismuth nano-particles between contacts with small separations and observed experimentally finite size effects associated with the power law predicted by equation (1). Atomic deposition and the subsequent growth of particles leading to an onset of conduction has been investigated in terms of percolation theory for Ag and In on Si(111) substrates by Heun et al. [18] and Takeda et al. [19] respectively.

3 Experimental procedure

Optical lithography was used to define NiCr/Au contacts (approximately 5 nm NiCr and 100 nm Au) on an insulating SiN epilayer on 3 mm × 3 mm pieces of Si substrate. The contact consisted of a ∼85 μm wide strip if NiCr/Au with a 70 μm rectangular gap missing from the conducting strip. Al wire was ultrasonically bonded to NiCr/Au strip to allow $I(V)$ measurements across the contacts to be taken prior to the deposition of the clusters to verify that there was minimal leakage current across the 70 μm gap. In all samples investigated the initial resistance between the contacts was measured and found to be in the ∼TΩ range.

During each deposition experiment a beam of particles was produced in an inert gas aggregation source [7]. Metal vapor was produced in the source chamber by heating bulk metal to 1200 °C, 850 °C and 760 °C for Ag, Bi and Sb respectively. Argon gas was fed into the source chamber to cool the metal vapor causing the aggregation of the vaporized atoms into nano-particles. The particles and argon were then extracted from the source chamber via a series of axially aligned exit nozzles, with increasingly high vacuum pumping stages between. Most of the argon was removed by the pumps, leaving a collimated beam of nano-particles, which entered the deposition chamber (base pressure $\approx 2 \times 10^{-6}$ Torr). Previously, electron diffraction patterns of particle beams produced by this source have been examined [20], and so the large particles produced by this system are known to have the crystal structure of the bulk material. A nominal deposition rate was determined using a quartz crystal film thickness monitor mounted in the beam path. The beam was then blocked by a mechanical shutter while the contacted sample ready for deposition was moved into place in the beam. 30 mV DC (previous studies in our group have shown that application of much larger voltages can

modify the structure and electrical characteristics of nano-particle films [21]) was applied across the electrical contacts; this voltage and the resulting current were recorded during the deposition. The particle beam produced a uniform spot ∼1.5 mm in diameter which was centered on the gap between the contacts.

After the deposition was completed the shutter was closed and the sample removed from the beam. The stability of the deposition rate during the experiment was then verified by measuring the deposition rate again. A second $I(V)$ measurement across the contacts was also made, and in all cases after deposition the deposited film showed Ohmic resistance with a considerably lower value than the contacts prior to deposition (see results and analysis below).

4 Results and analysis

Figure 1 compares the distribution of Bi, Ag and Sb nano-particles on the SiN substrates. Both the Bi and Ag nano-particles are distributed randomly on the SiN surface, whereas the Sb nano-particles tend to stick together in clumps separated by areas free of any particles. The atomic force microscope image (inset in Fig. 1 (top)) demonstrates that the Bi nano-particles form flattened dome shaped structures when deposited onto the substrate surface. The particles in the inset are somewhat larger than those in the main image which are ∼20 nm diameter on average, because it is easier to image the largest particles. Field emission scanning electron microscope (SEM) images (inset in Fig. 1 (middle)) taken from an acute observation angle show the Ag particles are tend to be spherical in shape, wetting the substrate to a lesser degree than the Bi particles. Again the particles in the inset are somewhat larger that the Ag particles in the main image (which are ∼15nm in diameter). There were occasional large hexagonal plates found amongst the silver particles, the distribution of these was sufficiently sparse so as to have no effect upon the percolation experiments. The distribution of both the Bi and Ag particles on the surface is random, and therefore closely matches the 2D Swiss cheese percolation model which is expected to hold for these materials, whereas for the Sb particles the distribution is very different and a simple percolation model would not be expected to apply. Field emission SEM images like Figure 1 (bottom) show that the Sb clusters tend to be spherical in shape (i.e., similar to the Ag clusters with a higher wetting angle than the Bi clusters), more regular in size and are ∼40 nm in diameter.

In these experiments the dimensions of the 2D region between the contacts where the particle film is deposited do not change and therefore the measured conductance is directly proportional to the conductivity of the system (prior to the transition to bulk film growth). The in situ electrical measurements were taken as a function of deposition time τ rather than coverage p. Therefore to facilitate the conversion from $\sigma(\tau)$ to $\sigma(p-p_c)$ it was assumed that the total coverage is directly proportional to the deposition time i.e. $p = k\tau$, and the critical coverage $p_c \approx 0.676$

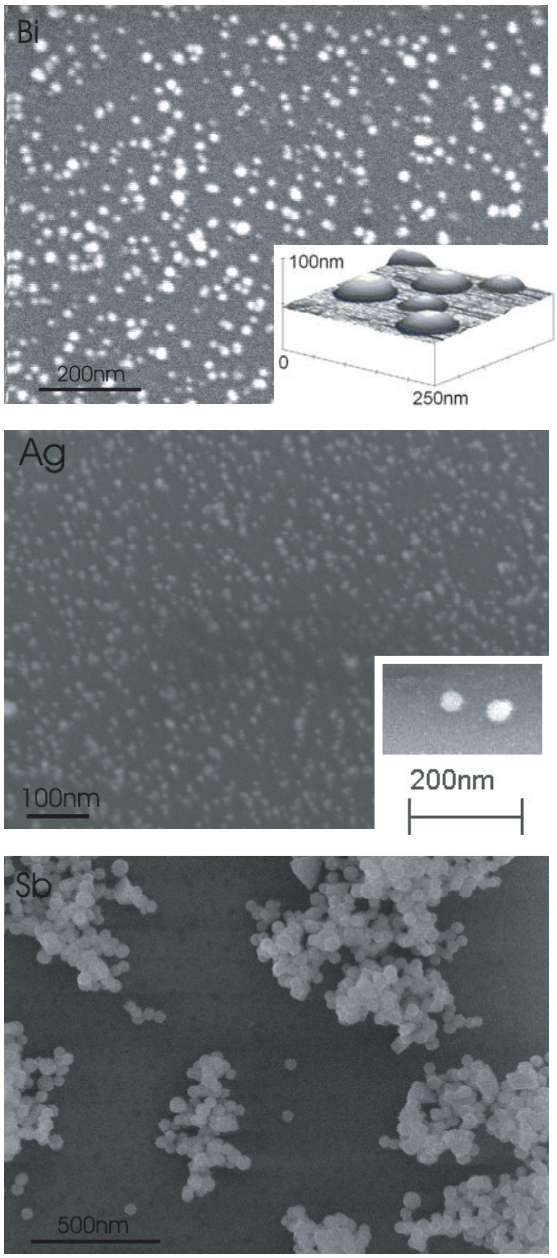

Fig. 1. Field emission SEM images of Bi nano-particles (top) and Ag nano-particles (middle) showing that the particles are randomly distributed on the SiN surface, and an image of Sb nano-particles (bottom) showing that the Sb particles are grouped together on the SiN surface in a non-random manner. The inset in the top image is an AFM close up of Bi nano-particles and the inset in the middle image is a field emission SEM close up of Ag particles taken at an oblique angle to highlight their spherical shape.

(theoretical value for a system of over lapping discs [9]) occurs at the critical time τ_c i.e., $p_c = k\tau_c$. The validity of this assumption is discussed further, later in this article.

Conductance onset measurements for two Bi nano-particle depositions are shown in Figure 2a. These conductance onset curves are similar to those recorded for Ag and Sb, shown in Figures 2b and 2c respectively. The

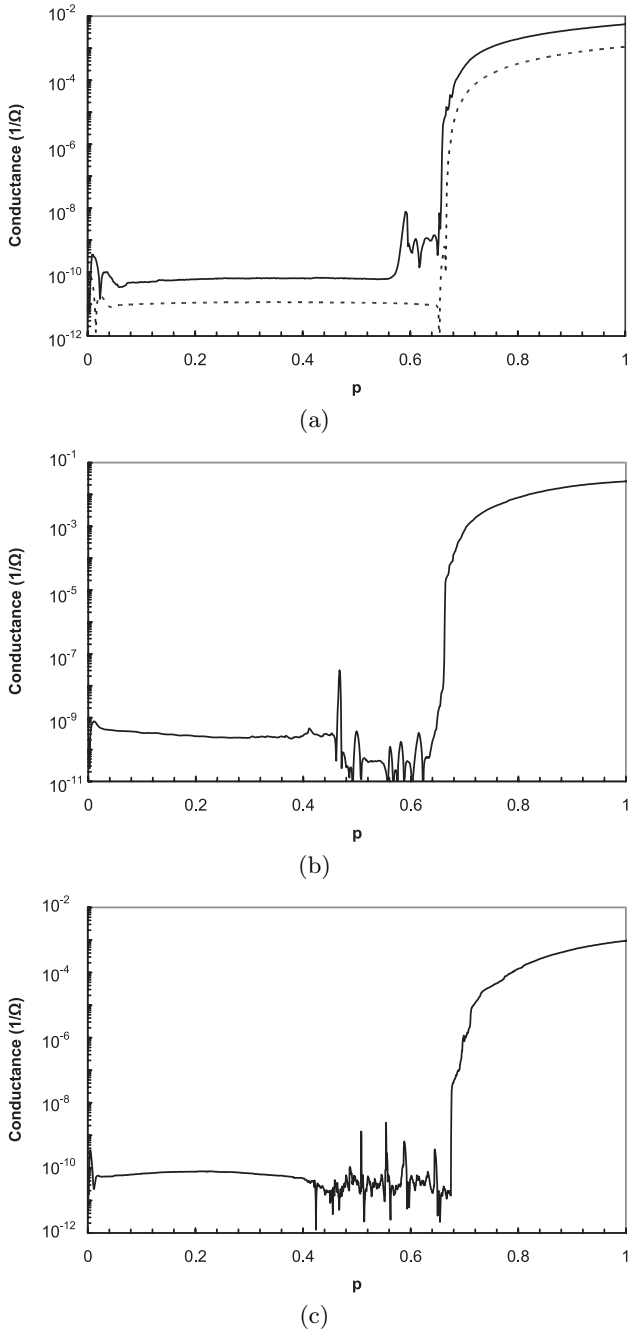

Fig. 2. Comparison of conductance onset curves for (a) two Bi depositions, (b) Ag deposition and (c) Sb deposition. In (a) the dashed line shows no pre-onset structure whereas the solid line (data multiplied by 10 to allow comparison between the two curves) is a current onset with pre-onset tunneling current.

structure in the conductance curve at very low coverage is an experimental artifact due to the electronic shutter opening. For all measurements in Figure 2 the initial conductance i.e., at low coverage, is very small ($\sim 10^{-10}\,\Omega^{-1}$), as expected since the theoretical conductivity of a percolating system is zero for $p < p_c$, and only increases for $p > p_c$. In all cases as the deposition continues the conductance increases very rapidly and changes by more than 5 orders of magnitude in $\sim$1 s (limited by the response time of the ammeter). Sometimes, although not always, this fast conductance increase is preceded by some structure in the conductance curve, as shown by the solid line in Figure 2a for Bi and in Figures 2b and 2c for Ag and Sb respectively. This structure prior to the sharp current onset is tentatively attributed to a tunneling current between particles which are separated by narrow regions of insulator (either an oxide layer or a narrow gap). The very fast increase in conductance at the onset time is due to the formation of a percolation pathway between the contacts via the deposited film. After the initial rapid increase in conductance there is a period of slower, steadily increasing conductance. It is this section of the curve which is of most interest since percolation theory predicts the conductance follows equation (2) for $p > p_c$. It should be noted that the conductance continues to increase after a complete layer of coverage has been achieved. By this stage the system has undergone a transition from filling a 2D layer to multilayer growth.

It is clear that a lower limit for the number of particles required to bridge the gap between the contacts can be calculated by dividing the separation between the contacts by the mean size of the deposited particles. This lower limit for the number of particles needed to span the gap between contacts is several thousand particles in the present experiments and therefore finite size effects are minimal [5,7], i.e. the percolation threshold should be very close to that for an infinite system. This latter point is an important consideration because the prediction of $t \approx 1.3$ from percolation theory is for an infinite system whereas experiments necessarily require finite systems. The mobility of the particles on the surface after impact is negligible due to their relatively large size (Ag$\sim$15 nm, Bi$\sim$20 nm and Sb$\sim$40 nm: equivalent to hundreds of thousands of atoms). A recent review outlines the criteria necessary for mobility for clusters up to a few thousand atoms [22].

Smith and Lobb [23] drew attention to the fact that close to the percolation threshold statistical fluctuations in the conductivity of a finite sample become large. They estimated the limit of the range of these fluctuations to be described by the condition $\xi \sim L$, where L is the system size i.e., $|p - p_c| \approx L^{-(1/\nu)}$. A similar approach was adopted by Dubson and Garland [15] who estimated the range of these fluctuations to be $\xi \sim L/2$ when fitting their data. Therefore, equation (2) was fitted to the experimental data in the range $0.006 < (p - p_c) < 0.324$. The lower limit is a conservative estimate of the coverage required such that $\xi \sim L$ and the upper limit is equivalent to complete coverage of the substrate. Initial attempts were made to fit the experimental data with a power law using the observed onset time τ_{onset} as the critical time τ_c; however this process did not yield satisfactory fits for the data. Percolation theory only determines the value of p_c for an infinite system and therefore necessarily finite individual experimental runs should yield a statistical distribution of values of τ_{onset} however these experiments were designed such that statistical variations due to the finite size of our sample area were minimized by keeping the

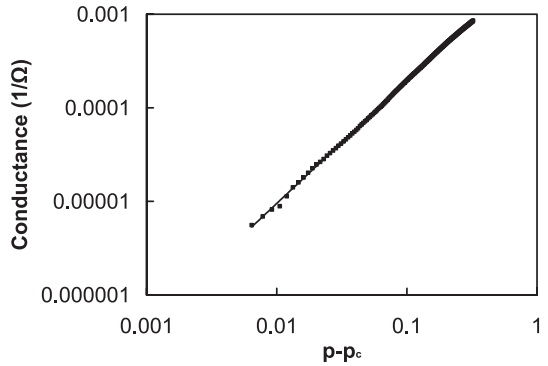

Fig. 3. An example of a power law (solid line) fitted to experimental conductance data (squares) for a bismuth deposition within the range $(p - p_c) = 0.006$ to 0.324. The formula of the resulting fit is $\sigma = 0.004\ (p - p_c)^{1.30}$.

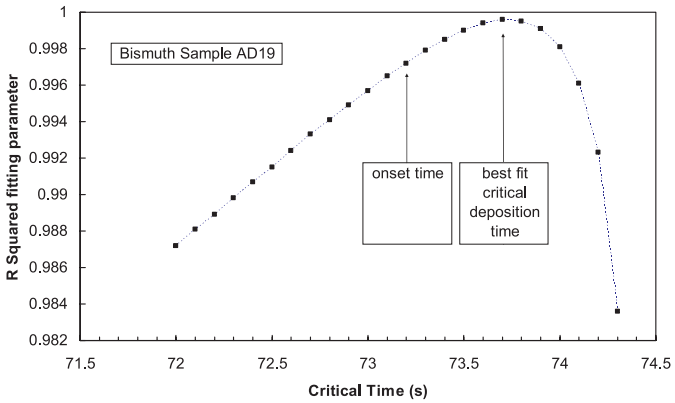

Fig. 4. A typical plot of the variation in the R^2 fitting parameter as the critical onset time is perturbed from the observed onset time. The best fit value of τ_c is taken at the maxima of this curve.

deposition area large in comparison to the particle size and therefore minimizing any statistical fluctuations between τ_c and τ_{onset}. Therefore other experimental factors such as variations in the surface water and hence oxidization rate of the nano-particles on the surface, oxidization of the particle traveling through the deposition chamber ($\sim 2 \times 10^{-6}$ Torr), small variations in the deposition rate during each deposition and non-uniformity of particle density across the beam, must be responsible for the run-to-run variations in these experiments. The upshot of these experimental factors is that in effect the assumption that $p = k\tau$ is not strictly true, but is instead only approximately true. Therefore the conductivity exponent for each experimental data set was determined by fitting a power law to each curve in the range $(p - p_c) = 0.006$ to 0.324 (see Fig. 3) using a sliding least squares fit which started with $\tau_c = \tau_{onset}$, and τ_c was then iteratively perturbed until the best least squares fit of equation (2) over the data range described above was achieved. Figure 4 shows a typical example of how the R^2 fitting parameter varies as the critical time is varied, the optimum value of τ_c for each data set being determined by the maxima in the value of

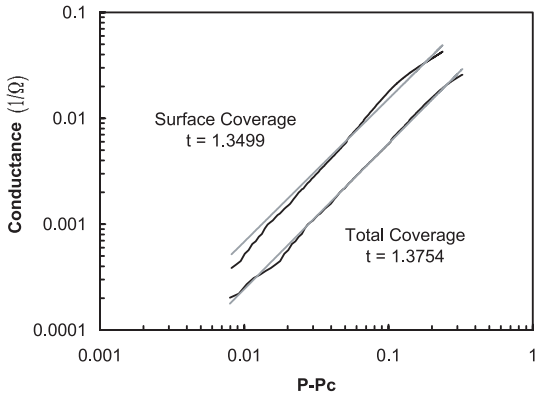

Fig. 5. Comparison of the values of t obtained from the uncorrected data and when the correction $p_{surface} = 1 - e^{-p}$ is applied for a typical deposition of Ag nano-particles.

R^2. It is noted that the choice of a sliding least squares fit for the data analysis is justified by the fact that the values of τ_c obtained from the sliding fit varied only slightly from the experimentally observed τ_{onset} values: for the Bi and Ag cluster experiments best fits were achieved when τ_c was within 6% of τ_{onset}.

Since the 2D theoretical model only considers a 2D layer on the surface over-lapping (or stacking) of the deposited particles has been considered. Stacking of particles leads to an under estimate of the true surface coverage in the conversion from $\sigma(\tau)$ to $\sigma(p - p_c)$ and will also cause an increase in the conductivity of the film because it is greater than one particle layer thick in some regions. Differential equations relating the probability of overlapping to the total coverage p (which is directly proportional to deposition time) and the surface coverage $p_{surface}$ were solved, yielding a relationship between the total coverage p and the surface layer coverage $p_{surface} = 1 - e^{-p}$. Implementing this correction to the coverage values used makes only a minor perturbation (<4%) for the fitted power law exponent t, as shown in Figure 5, which compares the t values for the surface coverage corrected data and the uncorrected total coverage data. The same sliding least squares fitting procedure as described above was used for both the corrected and uncorrected data in Figure 5. However, this correction only partially corrects for overlapping and does not take into account the fact that particle stacking in the experimental measurements will also result in an increase in conductivity due to the increased thickness of the stacked layer on the surface. This increase in the conductivity of the film due to stacked particles is not easily accounted for quantitatively but the influence of the relative conductivity increase on the exponent t is likely to be of the same order of magnitude as the correction for the coverage perturbation since both these effects stem from the over-lapping of particles. The two effects are relatively small and cause changes which have opposing effects on the conductivity and so for the purpose of this study they were neglected.

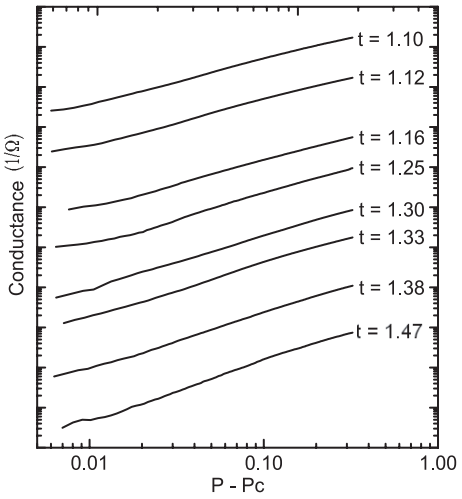

Fig. 6. The experimental conductance data for bismuth plotted as a function of $(p - p_c)$. The plots are stacked (each offset by an order of magnitude) in order of decreasing gradient. Only data points in the range $p = 0.006$ to 0.324 are shown and the exponent t from the fits for each data set is displayed at the end of each curve.

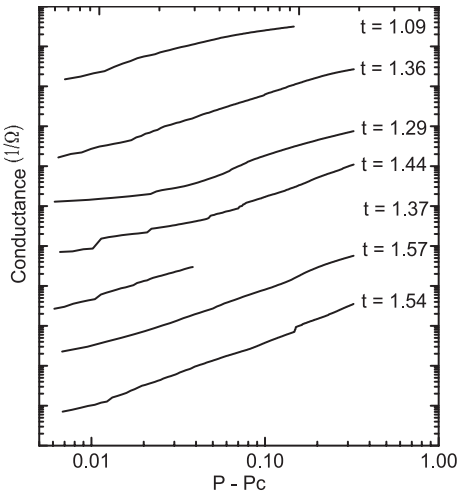

Fig. 7. The experimental conductivity data for Ag plotted as a function of $(p - p_c)$. Only data points in the range $p = 0.006$ to 0.324 are shown and the plots are stacked (each offset by an order of magnitude). The exponent t from the fits for each data set are displayed at the end of each curve.

4.1 Bismuth

The experimental data sets for eight bismuth depositions are shown in Figure 6, where each curve is vertically offset from the previous curve by an order of magnitude to allow clearer representation of the data. The eight results shown are for different experimental runs using identical system set up parameters and are shown to highlight the variations which occur between experimental runs. For Bi depositions, power curves closely fit the experimental data with an average value of the conductivity exponent of 1.27 ± 0.13, in close agreement with the theoretical value of 1.3.

The average exposure time before the sharp current onset for the Bi samples was 92 s for a nominal deposition rate of 0.02 nm/s and the average conductance when the 2D layer coverage was complete was 1.17 $\mathrm{m}\Omega^{-1}$ (or a resistance of 854 Ω).

4.2 Silver

Seven experimental data sets for Ag depositions are shown in Figure 7, where each curve is vertically offset from the previous curve by an order of magnitude. The seven results shown are for different experimental runs using identical system set-up parameters. The conductivity exponent for each experimental data set was determined as described and it was found that for Ag nano-particle depositions the power law equation (2) closely fits the experimental data with an average value of the conductivity exponent of 1.40 ± 0.14, also in reasonable agreement with the theoretical value of 1.3.

The average deposition time before the sharp current onset for the Ag films at a nominal deposition rate of 0.02 nm/s was 100 s and the Ag films had an average conductance of 10.9 $\mathrm{m}\Omega^{-1}$ (or a resistance of 92 Ω) when the coverage of 2D surface is complete.

4.3 Antimony

Experimental data collected during the antimony depositions, presented in Figure 8, was analyzed following the same procedure used for the Bi and Ag analysis. Once again the seven results shown are for different experimental runs using identical system set-up parameters and are shown to highlight the statistical variations which occur between runs. In general it was not possible to obtain a good fit to the Sb data with the power law equation (2) since the plots in Figure 7 are not linear. Values of t obtained for a few of the 'straighter' curves are included in Figure 7 for comparison with the Bi and Ag results.

The average time taken before current onset occurred for the Sb depositions was 256 s, and it was also noted that both the onset times and the deposition rates of the Sb clusters fluctuated greatly in comparison to the Ag and Bi depositions. The deposition times before the sharp current onset for Sb were found to range from times comparable with those found for Ag (average = 100 s) and Bi (average = 92 s) to values as high as 640 s. The average final conductance values obtained for the Sb analysis was 1.42 $\mathrm{m}\Omega^{-1}$ (or a resistance of 704 Ω).

5 Discussion

The Bi and Ag particles are randomly distributed on the SiN surface therefore the average switch on times for the Bi and Ag cluster depositions were similar, as expected for similar deposition rates. However it is noted that the final

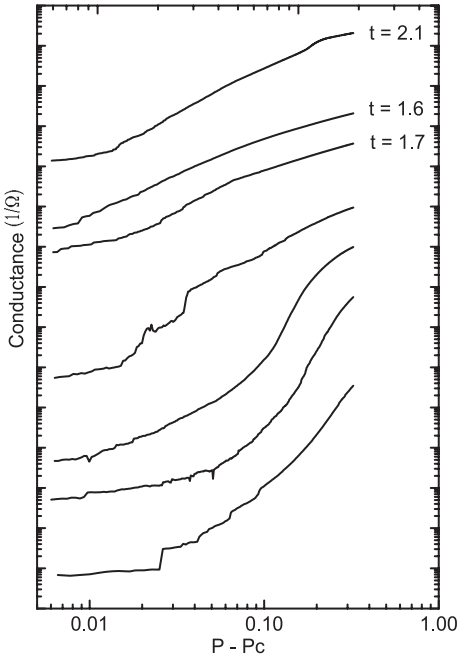

Fig. 8. The experimental conductivity data for antimony plotted as a function of $(p - p_c)$. The plots are stacked, each offset by an order of magnitude. Only data points in the range $p = 0.006$ to 0.324 are shown and the exponent t from the fits for the straightest data sets are displayed at the end of the associated curves.

conductance values of the Bi and Ag clusters are quite different, this is partially explained by the difference in bulk resistivity of the two materials (Bi: 117 $\mu\Omega$cm @ 20 °C and Ag: 1.6 $\mu\Omega$cm @ 20 °C). The average final resistance of the Ag cluster films (92 Ω) is approximately one order of magnitude less than that for Bi cluster films (854 Ω), however the bulk resistivity of Ag is close to two orders of magnitude less than that for Bi, therefore the difference in bulk resistivity cannot completely explain the differences. There are further complications due to differences in the packing of the Bi and Ag clusters and different oxidization rates for the two materials. The Bi clusters flatten to form dome shaped structures whereas the Ag clusters remain spherical resulting in differences in the size and distribution of the void regions within the final film.

The spread in the values of t reported for the Bi and Ag depositions is larger than is expected for a simple 2D percolating system where a universal value of t is predicted [10]. The presence of residual water, or other absorbents that could cause oxidization (and hence reduce the conductivity) of the nano-particles on the SiN surface at the relatively high vacuum pressures used has been considered. Since conduction onsets are observed it is clear that not all the particles are entirely oxidized, therefore it is assumed that any particles adhering to the surface will all be equally affected by oxidization effects and therefore the 2D Swiss cheese model should still describe the deposition process well, albeit with a lower final conductance for the deposited film. It should be noted that many of previously published experimental reports apply percolation theory to just a single deposition experiment and therefore do not provide any detail of the statistical spread. We include all our deposition data in order to emphasize the small differences between each experiment. Despite these run-to-run variations, by applying the sliding least squares fitting procedure to our experimental results, the mean value of the exponent t is still found to be in good agreement with percolation theory. Future experiments to deposit nano-particles in a UHV chamber and observe the conduction onset in a cleaner environment are planned.

The grouping together of the Sb nano-particles could be explained by (i) particles sticking together whilst in the beam and then impacting upon the surface in groups, or (ii) the Sb particles may be mobile on the substrate and move together after impact or (iii) the incident Sb particles strike the substrate in a random distribution, but only adhere to the surface when they impact upon a nucleation site or another cluster. Since nano-particles of the other materials do not stick together whilst in flight, and in any case, impact upon the surface would likely destroy any groups of particles which may have aggregated during flight, explanation (i) seems unlikely. As previously mentioned in the results and analysis section the relatively large size of the nano-particles in these experiments would suggest that significant mobility of the particles on the surface is also unlikely. Importantly, for the Sb depositions nano-particle material was observed on *both* sides of an aperture placed ∼2 mm in front of the substrate, whereas for the Ag and Bi depositions only the front face of this aperture had material deposited on it. Some of the Sb nano-particles bounce off the substrate and subsequently stick to the back side of the final aperture. Two other groups have also reported bouncing of Sb nano-particles [24] and this effect has recently been utilized in the production of Sb cluster assembled nanowires [25]. Therefore we propose that the non-random distribution of the Sb nano-particles is due to the majority of the particles bouncing off the substrate, unless they impact upon a suitable sticking site i.e. a surface defect or another nano-particle already stuck to the surface. Substrates from the same SiN wafer were used for all three materials, and hence there were no variations in surface quality.

The fact that the vast majority of the Sb nano-particles bounce off the substrate explains why for Sb there is a large increase in deposition time needed before the sharp increase in conduction occurs in most cases. The variation in Sb onset times from one experiment to the next can be explained by the variations in the number per unit area of defects from one sample to the next. If the number of defect sites where Sb particles can stick to the substrate is large the resulting onset time will be short. Similarly, if there are very few defects where the Sb can stick to the substrate the conduction onset time will be long. The exact nature of these defect sites is unknown and therefore their occurrence is an uncontrolled parameter in these experiments, resulting in the large variations in Sb conduction onset times.

The post onset electrical characteristics of the Sb particle depositions presented in Figure 7 are inconsistent with percolation theory; this is in contrast to reference [17] where 4.8 nm Sb clusters were deposited onto glass. The difference between reference [17] and the Sb data presented here may be due to differences in particle adhesion since different substrates, different sized particles and different impact energies were used. In reference [17] desorption of the Sb clusters used was reported to be negligible, whereas in this work there is strong evidence that a significant fraction of the Sb particles bounce off the SiN substrate.

Occasionally, step like structure was observed in some of the conductance data, particularly in the Ag data in Figure 6. It is thought that these steps occur when either the final clusters fall in place such that another percolating pathway is completed between the contacts and therefore suddenly increasing the total conductivity of the network, or, the one of the large hexagonal structures occasionally observed in the Ag films impacts upon the area between the electrical contacts.

6 Conclusions

The deposition of Bi and Ag nano-particles on 2D SiN surfaces results in randomly distributed films of nanoparticles. Therefore percolation theory can be used to describe onset of current flow through the resultant network. The average values of the conductivity power law exponent t for cluster depositions were found to be 1.27 ± 0.13 and 1.40 ± 0.14, for Bi and Ag respectively. These values are in agreement with the theoretical value of $t \approx 1.3$ predicted by percolation theory.

However, the conductivity increase during Sb nanoparticle depositions did not follow similar trends. The Sb particles did not adhere to the SiN substrate in a random distribution, instead the antimony particles were found to bounce off the substrate unless they impacted upon a suitable nucleation site or another Sb nano-particle stuck to the substrate. Therefore percolation theory could not be successfully used to model the onset of current flowing through a film of Sb nano-particles.

References

1. K. Meiwes-Broer, in *Metal Clusters at Surfaces* (Springer, Berlin, 2000)
2. P. Milani, S. Ianotta, in *Cluster Beam Synthesis of Nanostructured Materials* (Springer, Berlin, 1999)
3. F. Favier, E.C. Walter, M.P. Zach, T. Benter, R.M. Penner, Science **293**, 2227 (2001)
4. S.J. Tans, A.R.M. Verschueren, C. Dekker, Nature **393**, 49 (1998)
5. D. Stauffer, in *Introduction to Percolation Theory* (Taylor and Francis, London, 1985)
6. H.E. Stanley, Rev. Mod. Phys. **71**, S358 (1999)
7. J. Schmelzer Jr, S.A. Brown, A. Wurl, M. Hyslop, Phys. Rev. Lett. **88**, 226802-1 (2002)
8. B.J. Last, D.J. Thouless, Phys. Rev. Lett. **27**, 1719 (1971)
9. J. Quintanilla, S. Torquato, R.M. Ziff, J. Phys. A: Math. Gen. **33**, L399 (2000)
10. S. Feng, B.I. Halperin, P.N. Sen, Phys. Rev. B **35**, 197 (1987)
11. B.I. Halperin, S. Feng, P.N. Sen, Phys. Rev. Lett. **54**, 2391 (1985)
12. I. Balberg, Phys. Rev. B **57**, 13351 (1998)
13. A. Okazaki, K. Maruyama, K. Okumura, Y. Hasegawa, S. Miyazima, Phys. Rev. E **54**, 3389 (1996)
14. A. Okazaki, K. Horibe, K. Maruyama, S. Miyazima, Phys. Rev. E **61**, 6215 (2000)
15. M.A. Dubson, J.C. Garland, Phys. Rev. B **32**, 7621 (1985)
16. S. Yamamuro, K. Sumiyama, T. Hihara, K. Suzuki, J. Phys. Soc. Jap. **68**, 28 (1999)
17. P. Melinon, P. Jensen, Jian Xiong Hu, A. Hoareau, B. Cabaud, M. Treilleux, D. Guillot, Phys. Rev. B **44**, 12562 (1991)
18. S. Heun, J. Bange, R. Schad, M. Henzler, J. Phys.: Condens. Matter, **5** 2913 (1993)
19. S. Takeda, X. Tong, S. Ino, S. Hasegawa, Surf. Sci. **415**, 264 (1998)
20. A. Wurl, M. Hyslop, S.A. Brown, B.D. Hall, R. Monot, Eur. Phys. J. D **16**, 205 (2001)
21. M. Schulze, S. Gourley, S.A. Brown, A. Dunbar, J. Partridge, R.J. Blaikie, Eur. Phys. J. D **24**, 291 (2003)
22. C. Binns, Surf. Sci. Rep. **44**, 1 (2001)
23. L.N. Smith, C.J. Lobb, Phys. Rev. B **20**, 3653 (1979)
24. W. Harbich, B. von Issendorf, private communications
25. J.G. Partridge, S. Scott, A.D.F. Dunbar, M. Schulze, S.A. Brown, A. Wurl, R.J. Blaikie, IEEE Trans. Nanotech. **3**, 61 (2004)